

# Hall-like response from anisotropic Fermi surfaces

Abhiram Soori\*

*School of Physics, University of Hyderabad, C. R. Rao Road, Gachibowli, Hyderabad-500046, India.*

We demonstrate that an anisotropic and rotated Fermi surface can generate a finite Hall-like transverse response in electron transport, even in the absence of a magnetic field or Berry curvature. Using a two-dimensional continuum model, we show that broken  $k_y \rightarrow -k_y$  symmetry inherent to anisotropic band structures leads to a nonzero transverse conductivity. We construct a lattice model with direction-dependent nearest- and next-nearest-neighbor hoppings that faithfully reproduces the continuum dispersion and allows controlled rotation of the Fermi contour. Employing a multiterminal geometry and the Büttiker-probe method, we compute the resulting Hall voltage and establish its direct correspondence with the continuum transverse response. The effect increases with the degree of anisotropy and vanishes at rotation angles where mirror symmetry is restored. Unlike the quantum Hall effect, the Hall response predicted here is not quantized but varies continuously with the band-structure parameters. Our results provide a symmetry-based route to engineer Hall-like signals in low-symmetry materials without magnetic fields or topological effects.

## I. INTRODUCTION

Free-electron theory provides the simplest description of the electronic properties of metals [1, 2]. While this theory treats electrons as moving in a translationally invariant continuum, the actual electronic motion takes place on a lattice, a feature naturally captured by the tight-binding model. These two descriptions can be mapped onto each other. Within the free-electron framework, the dispersion takes the familiar parabolic form  $E = \hbar^2 k^2 / 2m - \mu$ , with an effective mass  $m$ . However, in several classes of materials—including layered semiconductors such as  $\text{ReSe}_2$  [3, 4] the dispersion becomes anisotropic, resulting in direction-dependent effective masses. Even in a two-dimensional electron gas (2DEG) with an originally circular Fermi surface, a series of periodically spaced barrier potentials can induce anisotropy and distort the Fermi contour [5, 6].

The Hall effect, in contrast, appears in several forms. The most familiar is the conventional Hall effect, where a transverse voltage develops in a 2DEG subjected to a perpendicular magnetic field [1, 2]. In the presence of Rashba spin-orbit coupling, an in-plane magnetic field may also generate a transverse response—the planar Hall effect—arising from the field-induced shift of the spin-orbit-coupled Fermi surface [7, 8]. These examples illustrate that transverse currents and Hall-like responses need not always originate from Lorentz forces; they can also be rooted in the geometry and symmetry of the Fermi surface.

In general, for an isotropic 2DEG with a circular Fermi surface, transverse currents cancel because states with opposite transverse momenta carry equal-and-opposite contributions. However, this cancellation breaks down when the crystallographic axes of a 2DEG with an anisotropic Fermi surface are rotated relative to the transport direction. In such a configuration, states with

opposite transverse momenta and identical longitudinal momentum need not exist, and a net transverse current can appear even without magnetic fields or broken time-reversal symmetry. Such an effect rooted in anisotropy of the Fermi contour has been studied in the context of Josephson junctions [9, 10].

In this work, we analyse this effect in detail. We first compute the transverse conductivity of a translationally invariant system with an anisotropic Fermi surface. We then examine the emergence of a Hall-like voltage in a lattice model of a 2DEG using the Büttiker-probe technique [11]. It is known that Hall voltage can appear in absence of time-reversal symmetry breaking due to reflection [12] or refraction [13] in the sample due to potential profile. Our results demonstrate that anisotropy and crystalline orientation is yet another way to generate transverse responses conventionally associated with Hall phenomena, despite the complete absence of magnetic fields or any mechanism that breaks time-reversal symmetry.

## II. CONTINUUM MODEL

In this section, we describe the system using a continuum model. The system is assumed to be translationally invariant along both  $\hat{x}$  and  $\hat{y}$  directions. Electrons are described within a free-electron framework but with direction-dependent effective masses, leading to an elliptical Fermi contour. The Hamiltonian is

$$H_c = -(t - \delta \cos 2\phi) a^2 \partial_x^2 - (t + \delta \cos 2\phi) a^2 \partial_y^2 + 2\delta \sin 2\phi a^2 \partial_x \partial_y, \quad (1)$$

where  $\delta$  denotes the anisotropy parameter and  $\phi$  specifies the angle between the major axis of the elliptical Fermi contour and the  $\hat{x}$  direction, and  $a$  is a length-scale that can be thought of as lattice spacing of the underlying lattice. For simplicity, we choose  $0 \leq \delta < t$ . In the

\* abhirams@uohyd.ac.in

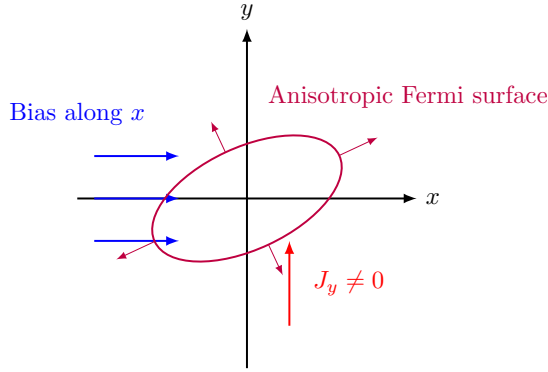


FIG. 1. A two-dimensional electron gas with an anisotropic band structure, translationally invariant along both directions, is subjected to a bias applied along  $\hat{x}$ . The elliptical Fermi contour is rotated such that its major axis is misaligned with both  $\hat{x}$  and  $\hat{y}$ . The red arrows denote the direction of the quasiparticle velocity on the contour. As a consequence of this misalignment, a longitudinal bias along  $\hat{x}$  generates a net transverse current along  $\hat{y}$ .

limiting case  $\delta = 0$ , the Fermi contour becomes isotropic, corresponding to an effective mass  $\hbar^2/2t$ .

The charge current density  $\vec{J} = (J_x, J_y)$  carried by a state with wavevector  $\vec{k} = (k_x, k_y)$  is given by

$$\begin{aligned} J_x &= 2e[(t - t_0 \cos 2\phi)k_x - \delta \sin 2\phi k_y]a^2/\hbar, \\ J_y &= 2e[(t + \delta \cos 2\phi)k_y - \delta \sin 2\phi k_x]a^2/\hbar. \end{aligned} \quad (2)$$

For a given energy  $E$ , the wavevector components may be parametrised by an angular parameter  $\theta$  as

$$\begin{aligned} k_x a &= \sqrt{E} \left[ \frac{\cos \theta \cos \phi}{\sqrt{t - \delta}} - \frac{\sin \theta \sin \phi}{\sqrt{t + \delta}} \right], \\ k_y a &= \sqrt{E} \left[ \frac{\cos \theta \sin \phi}{\sqrt{t - \delta}} + \frac{\sin \theta \cos \phi}{\sqrt{t + \delta}} \right], \end{aligned}$$

with  $\theta \in [0, 2\pi]$ . When  $\delta = 0$ , the parameter  $\theta$  reduces to the usual polar angle of  $\vec{k}$  measured from  $\hat{x}$ . It can be shown that  $J_x$  is positive for  $-\pi/2 - \eta < \theta < \pi/2 - \eta$ , where

$$\eta = \tan^{-1} \left[ \tan \phi \sqrt{\frac{t + \delta}{t - \delta}} \right].$$

Within the Landauer framework, applying a forward bias populates all states with positive longitudinal velocity. The longitudinal differential conductivity at bias  $V = E/e$  is therefore

$$G_{xx} = \frac{e}{8\pi^2 a \sqrt{t^2 - \delta^2}} \int_{-\pi/2 - \eta}^{\pi/2 - \eta} J_x(E, \theta) d\theta. \quad (3)$$

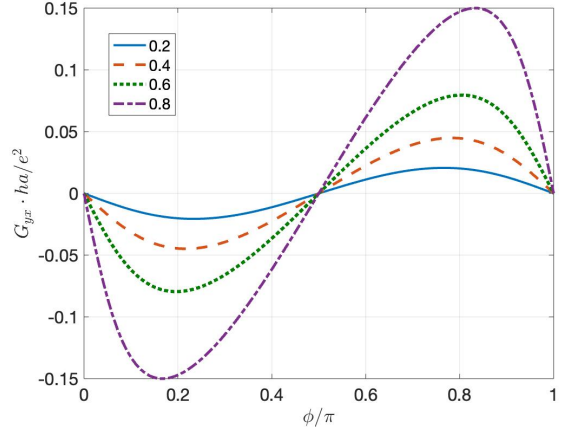


FIG. 2. Transverse conductivity as a function of the angle between the major axis of the elliptical Fermi contour and the longitudinal bias direction ( $\hat{x}$ ). Different curves correspond to different values of the anisotropy ratio  $\delta/t$  (shown in the legend).

The transverse differential conductivity quantifies the net transverse current  $I_y$  generated by a longitudinal bias  $V$ . It is defined as  $dI_y/dV$ , and is given by

$$G_{yx} = \frac{e}{8\pi^2 a \sqrt{t^2 - \delta^2}} \int_{-\pi/2 - \eta}^{\pi/2 - \eta} J_y(E, \theta) d\theta. \quad (4)$$

Evaluating the integral yields

$$G_{yx} = -\frac{e^2}{\pi ha} \sqrt{\frac{2E(t + \delta \cos 2\phi)}{t^2 - \delta^2}} \sin(\eta - \eta'), \quad (5)$$

$$\text{where } \eta' = \tan^{-1} \left[ \tan \phi \sqrt{\frac{t - \delta}{t + \delta}} \right].$$

At  $\phi = 0$  and  $\phi = \pi/2$ , one finds  $\eta = \eta'$ , and consequently the transverse conductivity vanishes. The behaviour of  $G_{yx}$  as a function of  $\phi$ , the angle between the major axis of the elliptical Fermi contour and the bias direction  $\hat{x}$ , is shown in Fig. 2.

### III. LATTICE MODEL

A square lattice with anisotropic nearest-neighbor hoppings is the simplest model that captures an anisotropic band structure. However, when the resulting Fermi surface is rotated, forming junctions with other materials becomes difficult. To overcome this, one may consider a two-dimensional square lattice with both nearest-neighbor and next-nearest-neighbor hoppings, which allows the anisotropic band structure to be rotated by tuning suitable parameters [14]. We first study such a lattice model for an anisotropic band structure, as shown in the

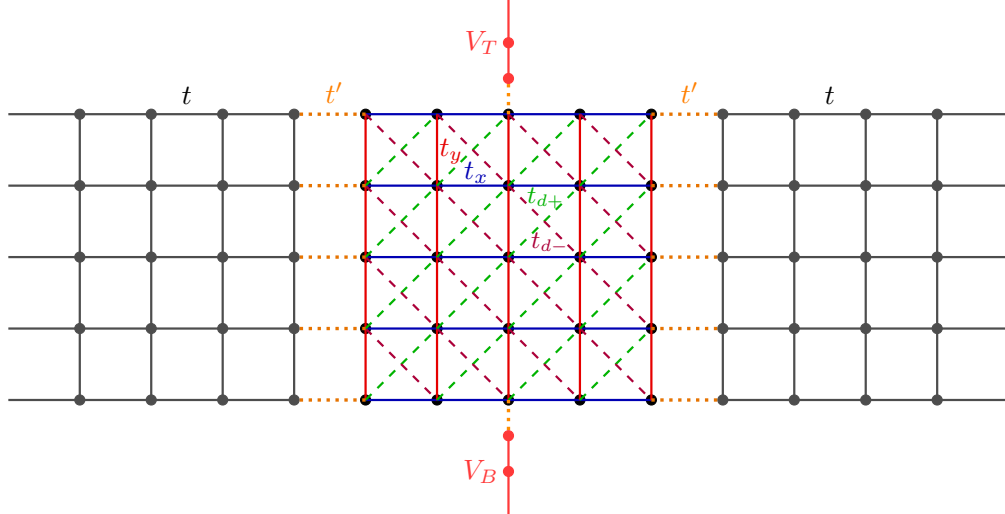


FIG. 3. Schematic of the lattice-based setup used to probe the Hall response arising from an anisotropic Fermi contour. The central region is a square lattice with direction-dependent nearest- and next-nearest-neighbor hopping amplitudes, connected to source and drain terminals on either side. Two voltage probe terminals are attached symmetrically along the transverse direction. A bias voltage  $V$  applied between the source and drain drives a longitudinal current, while the transverse voltage difference  $V_H$  that develops between the probe terminals quantifies the Hall-like response. See the Hamiltonian in Eq. (9) for details.

central region of Fig. 3. The model can be written as

$$\begin{aligned}
 H_l = & -t_x \sum_{n_x, n_y} c_{n_x+1, n_y}^\dagger c_{n_x, n_y} - t_y \sum_{n_x, n_y} c_{n_x, n_y+1}^\dagger c_{n_x, n_y} \\
 & -t_+ \sum_{n_x, n_y} c_{n_x+1, n_y+1}^\dagger c_{n_x, n_y} - t_- \sum_{n_x, n_y} c_{n_x-1, n_y+1}^\dagger c_{n_x, n_y} \\
 & + \text{h.c.},
 \end{aligned} \tag{6}$$

where  $t_x$  and  $t_y$  are nearest-neighbour hopping amplitudes along  $x$  and  $y$  directions, and  $t_+$  and  $t_-$  are the next-nearest-neighbour hopping amplitudes along  $\hat{x} + \hat{y}$  and  $\hat{x} - \hat{y}$  directions respectively. The operator  $c_{n_x, n_y}$  annihilates an electron on site  $(n_x, n_y)$ . The hopping amplitudes are taken to be real for simplicity. The dispersion relation for this model is given by

$$\begin{aligned}
 E = & -2[t_x \cos k_x a + t_y \cos k_y a \\
 & + t_+ \cos (k_x + k_y) a + t_- \cos (k_x - k_y) a]
 \end{aligned} \tag{7}$$

It can be shown that a Taylor expansion of this dispersion near  $k_x = k_y = 0$  reproduces the continuum dispersion

(up to an overall energy shift) obtained from the Hamiltonian in Eq. (1), provided the lattice parameters are chosen such that

$$\begin{aligned}
 t_x &= t - \delta \cos 2\phi, \quad t_y = t + \delta \cos 2\phi, \\
 \text{and } t_+ &= -t_- = -\delta \sin 2\phi.
 \end{aligned} \tag{8}$$

We now consider a realistic setup in which the Hall response can be experimentally probed. Source and drain terminals are attached to the left and right edges of the lattice hosting the anisotropic band structure. In addition, two probe terminals—each modeled as a one-dimensional quantum wire—are connected symmetrically along the transverse (up and down) directions to the same lattice, as illustrated in Fig. 3. We calculate Hall-voltage using the probe terminals in response to a bias in longitudinal direction using Büttiker probe technique [11].

The Hamiltonian for the setup shown in Fig. 3 is given by

$$H = H_L + H_M + H_R + H_T + H_B + H_{LM} + H_{MR} + H_{TM} + H_{BM},$$

where

$$H_L = -t \left[ \sum_{n_x=-\infty}^0 \sum_{n_y=1}^{L_y} c_{n_x-1, n_y}^\dagger c_{n_x, n_y} + \sum_{n_x=-\infty}^0 \sum_{n_y=1}^{L_y-1} c_{n_x, n_y+1}^\dagger c_{n_x, n_y} \right] + \text{h.c.} - \mu_L \sum_{n_x=-\infty}^0 \sum_{n_y=1}^{L_y} c_{n_x, n_y}^\dagger c_{n_x, n_y},$$

$$\begin{aligned}
H_M &= -t_x \sum_{n_x, n_y} c_{n_x+1, n_y}^\dagger c_{n_x, n_y} - t_y \sum_{n_x, n_y} c_{n_x, n_y+1}^\dagger c_{n_x, n_y} - t_+ \sum_{n_x, n_y} c_{n_x+1, n_y+1}^\dagger c_{n_x, n_y} - t_- \sum_{n_x, n_y} c_{n_x-1, n_y+1}^\dagger c_{n_x, n_y} \\
&\quad + \text{h.c.} - \mu_M \sum_{n_x=1}^{L_x} \sum_{n_y=1}^{L_y} c_{n_x, n_y}^\dagger c_{n_x, n_y}, \\
H_R &= -t \left[ \sum_{n_x=L_x+1}^{\infty} \sum_{n_y=1}^{L_y} c_{n_x+1, n_y}^\dagger c_{n_x, n_y} + \sum_{n_x=L_x+1}^{\infty} \sum_{n_y=1}^{L_y-1} c_{n_x, n_y+1}^\dagger c_{n_x, n_y} \right] + \text{h.c.} - \mu_R \sum_{n_x=L_x+1}^{\infty} \sum_{n_y=1}^{L_y} c_{n_x, n_y}^\dagger c_{n_x, n_y}, \\
H_T &= -t \sum_{n=1}^{\infty} (d_{n+1}^\dagger d_n + \text{h.c.}) - \mu_P \sum_{n=1}^{\infty} d_n^\dagger d_n, \quad H_B = -t \sum_{n=-\infty}^{-1} (d_{n-1}^\dagger d_n + \text{h.c.}) - \mu_P \sum_{n=-\infty}^{-1} d_n^\dagger d_n, \\
H_{LM} &= -t' \sum_{n_y=1}^{L_y} (c_{0, n_y}^\dagger c_{1, n_y} + \text{h.c.}), \quad H_{MR} = -t' \sum_{n_y=1}^{L_y} (c_{L_x, n_y}^\dagger c_{L_x+1, n_y} + \text{h.c.}), \\
H_{TM} &= -t_P (d_1^\dagger c_{n_{x0}, L_y} + \text{h.c.}), \quad H_{BM} = -t_P (d_{-1}^\dagger c_{n_{x0}, 1} + \text{h.c.}) . \tag{9}
\end{aligned}$$

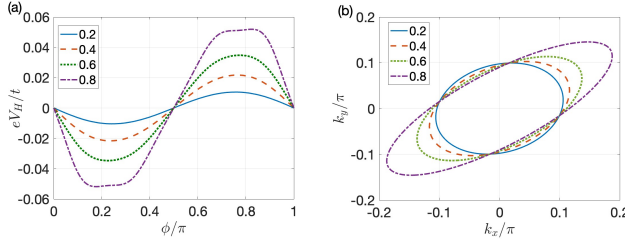


FIG. 4. (a) Hall voltage as a function of  $\phi$ , the angle of rotation of the system. Parameters:  $L_x = L_y = 11$ ,  $n_{x0} = 6$ ,  $\mu_n = -2t$ ,  $\mu_M = -4t$ ,  $t' = t$ ,  $t_P = 0.05t$ , and  $eV = 0.1t$ . Different curves correspond to different values of  $\delta$ . (b) Fermi contour of the central lattice for various choices of  $\delta$  at energy  $0.1t$ . The legends indicate the values of  $\delta/t$ .

Here,  $\mu_L$  and  $\mu_R$  denote the chemical potentials of the source and drain terminals, respectively, and are taken to be equal,  $\mu_L = \mu_R = \mu_n$ . The central square lattice with anisotropic band structure has chemical potential  $\mu_M$ . The operator  $d_n$  annihilates an electron on site  $n$  of a probe terminal. The hopping amplitude connecting the anisotropic central lattice to the left and right terminals is denoted by  $t'$ , while the hopping amplitude linking the central lattice to the probe terminals is  $t_P$ .

We now briefly outline the method of calculation. The scattering eigenfunction corresponding to an electron incident in the  $m_0$ -th channel of the source at energy  $E$  is first obtained using standard scattering theory. This eigenfunction is then used to compute the currents flowing into the probe terminals. The total current through each probe terminal due to a longitudinal bias  $V$  is obtained by summing the contributions from all incident channels within the bias window. Next, scattering eigenfunctions for electrons incident from each of the probe terminals are computed, and the corresponding currents

are evaluated for a wide range of voltage pairs  $(V_T, V_B)$  applied at the probe terminals. The total currents in the probe terminals thus include contributions from the source-drain bias  $V$  as well as from the applied probe-terminal voltages. From the set of sampled voltage pairs, we identify those for which the net current in both probe terminals vanishes. The corresponding voltage difference  $V_T - V_B$  defines the Hall voltage  $V_H$ . All calculations are performed numerically.

In Fig. 4(a), we plot the transverse voltage  $V_H$  as a function of the rotation angle  $\phi$  for  $L_x = L_y = 11$ ,  $n_{x0} = 6$ ,  $\mu_n = -2t$ ,  $\mu_M = -4t$ ,  $t' = t$ ,  $t_P = 0.05t$ , and  $eV = 0.1t$ . As the anisotropy parameter  $\delta$  increases, the magnitude of the transverse voltage grows, since the symmetry  $k_y \rightarrow -k_y$  is increasingly broken at larger  $\delta$ . Furthermore, at  $\phi = 0, \pi/2, \pi$ , the transverse voltage vanishes because the Fermi surface regains symmetry under  $k_y \rightarrow -k_y$ . Figure 4(b) shows the Fermi contour of the central lattice at  $\phi = 0.3\pi$  for different values of  $\delta/t$ .

#### IV. DISCUSSION AND CONCLUSION

We have predicted a Hall-like transverse response in electron transport through a metal with an anisotropic band structure, even in the absence of a magnetic field or Berry curvature. Using a two-dimensional continuum model that is translationally invariant in both directions, we demonstrated that an anisotropic and rotated Fermi contour naturally leads to a finite transverse conductivity.

To connect this continuum picture to a realistic mesoscopic setup, we constructed a corresponding lattice model with direction-dependent nearest- and next-nearest-neighbor hoppings. This lattice model faithfully reproduces the desired continuum dispersion and, importantly, allows controlled rotation of the anisotropic

band structure by tuning a small set of microscopic parameters. We then attached source and drain terminals along the longitudinal direction and voltage-probe terminals along the transverse direction, forming a multiterminal transport geometry suitable for numerical study. Using the Büttiker-probe method, we computed the Hall voltage generated across the transverse probes and established that it tracks the underlying transverse conductivity obtained from the continuum model.

Our results show that the magnitude of the Hall-like response is directly governed by the degree of anisotropy in the Fermi contour and its lack of symmetry under  $k_y \rightarrow -k_y$ . The response vanishes at specific rotation angles where this symmetry is restored. These features provide clear experimental signatures that can be tested in mesoscopic devices where strain can be possibly used to tune anisotropy. Importantly, unlike the quantum Hall effect [15], the Hall response predicted here is *not quantized*; rather, it is a continuous function of the anisotropy and the rotation angle of the Fermi surface.

Altermagnets provide a natural platform featuring intrinsically anisotropic band structures [16, 17]. However, the dispersions for the two spin species in altermagnets are rotated by  $90^\circ$  relative to each other in the  $k_x - k_y$  plane. Consequently, to access the effects presented in this work, one must use ferromagnetic source and drain electrodes so that transport is dominated by electrons of a single spin species. Thus, our predictions provide an experimentally relevant transport probe of al-

termagnetic anisotropy, potentially complementing spectroscopic studies.

Beyond altermagnets, our work highlights a broader principle: anisotropy combined with Fermi-surface rotation can mimic aspects of Hall physics without requiring magnetic fields or topological Berry-curvature effects. This opens a route to engineer Hall-like signals in a wide class of low-symmetry materials, including strained metals, anisotropic two-dimensional materials, and artificial lattices.

In summary, we have shown that anisotropic band structures with tunable orientation lead to a robust and measurable Hall-like transverse response. Our study provides a unified continuum and lattice framework to analyze this phenomenon, identifies its symmetry origins, and proposes realistic device geometries for its experimental detection. We hope our findings stimulate further exploration of anisotropy-driven transport effects in emergent materials.

## ACKNOWLEDGMENTS

The author thanks Gajanan V Honnavar, Manisha Thakurathi and Dhavala Suri for useful discussions. The author thanks Science and Engineering Research Board (now Anusandhan National Research Foundation) - Core Research grant (CRG/2022/004311) and University of Hyderabad for financial support.

- 
- [1] C. Kittel, *Introduction to Solid State Physics* (Wiley India, Noida, 2004).
- [2] N. W. Ashcroft and N. D. Mermin, *Solid State Physics* (Holt-Saunders, 1976).
- [3] Y.-C. Lin, H.-P. Komsa, C.-H. Yeh, T. Björkman, Z.-Y. Liang, C.-H. Ho, Y.-S. Huang, P.-W. Chiu, A. V. Krasheninnikov, and K. Suenaga, Single-layer  $\text{ReS}_2$ : Two-dimensional semiconductor with tunable in-plane anisotropy, *ACS Nano* **9**, 11249 (2015).
- [4] X. Liu, Y. Yuan, Z. Wang, R. S. Deacon, W. J. Yoo, J. Sun, and K. Ishibashi, Directly probing effective-mass anisotropy of two-dimensional  $\text{re}_2$  in schottky tunnel transistors, *Phys. Rev. Applied* **13**, 044056 (2020).
- [5] K. Ismail, W. Chu, D. A. Antoniadis, and H. I. Smith, Surface-superlattice effects in a grating-gate  $\text{GaAs}/\text{GaAlAs}$  modulation doped field-effect transistor, *Applied Physics Letters* **52**, 1071 (1988).
- [6] C. W. J. Beenakker and H. van Houten, Quantum transport in semiconductor nanostructures, in *Semiconductor Heterostructures and Nanostructures*, Solid State Physics, Vol. 44, edited by H. Ehrenreich and D. Turnbull (Academic Press, 1991) pp. 1–228.
- [7] N. Wadehra, R. Tomar, R. M. Varma, R. K. Gopal, Y. Singh, S. Dattagupta, and S. Chakraverty, Planar Hall effect and anisotropic magnetoresistance in polar-polar interface of  $\text{LaVO}_3 - \text{KTaO}_3$  with strong spin-orbit coupling, *Nat. Commun.* **11**, 874 (2020).
- [8] A. Soori, Finite transverse conductance and anisotropic magnetoconductance under an applied in-plane magnetic field in two-dimensional electron gases with strong spin-orbit coupling, *J. Phys.: Condens. Matter* **33**, 335303 (2021).
- [9] B. K. Sahoo and A. Soori, Four-terminal josephson junctions: diode effects, anomalous currents and transverse currents, *J. Phys.: Condens. Matter* **37**, 305302 (2025).
- [10] S. Mazumdar, A. Mukherjee, K. Saha, and S. Das, Enhanced andreev reflection in flat-band systems: Wave packet dynamics, dc transport and the josephson effect (2025), arXiv:2507.06327 [cond-mat.supr-con].
- [11] A. Soori and U. Khanna, Decoherence in electron transport: back-scattering, effect on interference and rectification, *Physica Scripta* **99**, 115957 (2024).
- [12] A. M. Song, A. Lorke, A. Kriele, J. P. Kotthaus, W. Wegscheider, and M. Bichler, Nonlinear electron transport in an asymmetric microjunction: A ballistic rectifier, *Phys. Rev. Lett.* **80**, 3831 (1998).
- [13] R. Sarkar, A. Bandyopadhyay, A. Narayan, and D. Sen, Refraction Hall effect (2025), arXiv:2511.15337 [cond-mat.mes-hall].
- [14] L. Sharma and M. Thakurathi, Tunable josephson diode effect in singlet superconductor-altermagnet-triplet superconductor junctions, *Phys. Rev. B* **112**, 104506 (2025).
- [15] K. v. Klitzing, G. Dorda, and M. Pepper, New method for high-accuracy determination of the fine-structure constant based on quantized Hall resistance, *Phys. Rev. Lett.*

- 45, 494 (1980).
- [16] L. Šmejkal, J. Sinova, and T. Jungwirth, Emerging research landscape of altermagnetism, *Phys. Rev. X* **12**, 040501 (2022).
- [17] C. Song, H. Bai, Z. Zhou, L. Han, H. Reichlova, J. H. Dil, J. Liu, X. Chen, and F. Pan, Altermagnets as a new class of functional materials, *Nature Reviews Materials* **10**, 473 (2025).